Experimental Synchronization of Spatiotemporal Disorder

R. Neubecker and B. Gütlich

Institute of Applied Physics, Darmstadt University of Technology, Hochschulstrasse 6, 64289 Darmstadt, Germany

(Received 28 April 2003; published 15 April 2004)

We report experimental evidence of a time-lag synchronization of spatiotemporal complexity. The experiments were performed on two unidirectionally coupled, nonlinear-optical systems of single-feedback type. Synchronization was investigated for different degrees of complexity of the spontaneous structures, which were analyzed with cross-correlation functions and mutual information. Numerical simulations yield comparable results and throw a light on the impeding role of spatial inhomogeneities.

DOI: 10.1103/PhysRevLett.92.154101 PACS numbers: 05.45.Xt, 42.65.Sf, 47.54.+r, 89.75.Kd

It is well known that two coupled chaotic oscillators can synchronize [1]. A new topic is the expansion of this concept to extended systems, regarding coupling-induced correspondence of complex states in time and in space. Such complex spatial structures, which spontaneously form in extended nonlinear systems, play a role in many fields, from biology over chemistry to areas of physics [2], e.g., fluid dynamics or nonlinear optics [3].

To achieve synchronization, the two regarded systems must communicate. In most pattern forming systems, the experimental realization of this coupling is difficult. The spatial distribution of physical quantities, such as a flow field or the concentration of chemical compounds, must be manipulated dynamically by injecting a coupling signal. Therefore, until now only numerical simulations of prototype models are performed, mostly in one spatial dimension only [4–6]. Both unidirectional and bidirectional coupling and the synchronization of not completely identical systems were investigated [5]. Since the communication of the full spatial distribution of a system state is considered to be problematic, often only few discrete coupling channels were used [6]. We instead regard the coupling of the full, space-continuous, and time-continuous state of spatially two-dimensional systems.

Light waves are ideal to realize the coupling signal, since they can carry almost arbitrary spatial and temporal profiles. Hence, it is straightforward to use a nonlinear-optical system, where the light field is already a central physical quantity. Our experimental setup belongs to the class of the so-called *single-feedback systems*, which have attracted growing attention [7–12].

In our system, a liquid crystal light valve (LCLV) is used as optical nonlinearity, providing a self-defocusing, saturable Kerr-type nonlinearity. The LCLV consists of two thin layers, separated by a mirror. The layers are sandwiched between two transparent, unstructured electrodes to which a supply voltage is applied [13]. One layer is a photoconductor (PC), which changes its conductivity according to the intensity profile $I_w(x, y)$ of an incident light wave. This results in a space dependent voltage drop over the other layer, a liquid crystal (LC), affecting its effective refractive index. A light wave, which passes the LC layer (*read side*) and is internally reflected, consequently acquires a transverse phase profile, which is determined by the intensity profile at the PC (*write side*).

The LCLV is operated under optical feedback: A plane pump wave is phase modulated and reflected by the LCLV read side. The modulated wave is then fed back to the write side by beam splitters (BS), mirrors (M), and lenses (L), as shown in Fig. 1. During the propagation through the feedback loop, the phase profile is converted into an intensity modulation by diffraction, thus closing the feedback. For detection purposes, a fraction of the feedback wave is coupled out with the beam splitter BS2. We use a digital camera to record an intensity distribution $I_w(x, y, t)$ equivalent to the one at the LCLV's write side. More details about this system and the theoretical modeling can be found in [10,11]. Because of their versatility, LCLV systems are frequently used to investigate spontaneous optical structures. In contrast to other configurations with a rotation or a lateral shift of the feedback wave [9,12], in our spatially symmetric system the dominant spatial coupling is provided by diffraction.

Above a threshold I_{th} of the pump intensity I_p, the plane-wave state becomes modulationally unstable with respect to a critical transverse wave number k_c. At higher respective thresholds, also higher order critical wave numbers become unstable. Increasing the pump intensity

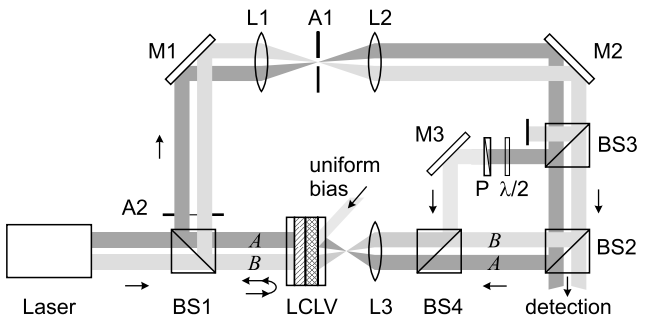

FIG. 1. Schematic experimental setup. For clarity, the pump beam is always drawn as the two beams of the subsystems *A* and *B*. Components for beam expansion, for detection, and for the generation of the bias beam are left out for simplicity.

from below threshold, first a stationary hexagonal pattern develops [7,10], and then the patterns become increasingly disordered [14,15]. Our system contains a spatial low-pass filter in the feedback (aperture A1, lenses L1, L2). By setting the low-pass cutoff just above the first critical wave number, the evolution of spatial disorder is attenuated and the degree of complexity grows more smoothly with the pump intensity [15,16].

Snapshots of experimentally observed structures are shown in Figs. 2 and 3. Just above threshold and with the low-pass filter closed, remainders of perfect order are visible as (moving) hexagonal domains, the typical extension of which shrinks with pump intensity. At 3 times threshold, mainly disordered arrangements of spotlike structures remain (not shown). With an open low-pass filter instead, pronounced disorder sets in already closely above threshold. Hence, the closed low pass allows us a finer adjustment of the degree of complexity. We found spatial complexity to be closely connected to temporal complexity, i.e., the more the pattern is spatially disordered, the more pronounced its dynamics.

We have recently shown how this system can be synchronized by injecting perfect hexagonal patterns [17]. The question addressed here is whether a synchronization in space and time can also be realized for spatiotemporal disorder. For this purpose, we regard two systems, one of which runs autonomously (master A), while the other (slave B) is exposed to the attenuated signal generated by the master system. Since it is difficult to get two identical LCLVs, we divided the active area of a single LCLV into two independent subsystems by inserting a mask A2 with two circular holes (diameters $D = 4$ mm). Because of inhomogeneities of the LCLV, the two systems A and B cannot be expected to be perfectly identical.

In the feedback, a fraction of the light waves was extracted with the beam splitter BS3. While the extracted signal from the slave system B was blocked, the wave from the master A was injected into B with the beam splitter BS4. A half-wave plate $\lambda/2$ and a polarizer P were used to attenuate the injected signal, i.e., to set the coupling factor γ. The perpendicular polarization behind the polarizer prevented interference effects. The recorded intensity distributions do not contain this coupling signal, because it was injected behind beam splitter BS2.

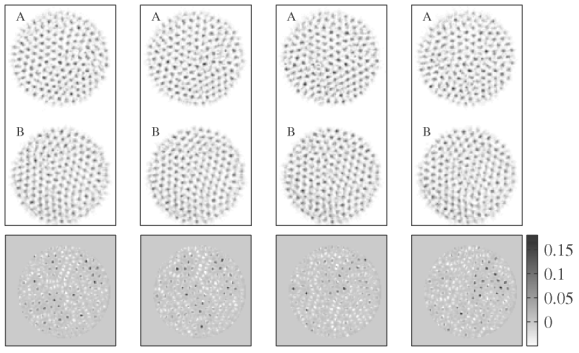

FIG. 2. Top: Snapshots from the recorded pattern sequence without coupling ($\gamma = 0$) in inverse gray scale (dark corresponds to high intensity). A and B denote master and slave systems, respectively. The system runs at a 1.5 times pattern forming a threshold with a closed low-pass filter; the images are taken at time intervals of $t = 2.6$ s. Bottom: the product of the intensity variations $\tilde{I}_A \cdot \tilde{I}_B$ visualizes the small local correlation. In the gray scale, zero corresponds to a shade of light gray, because anticorrelations $\tilde{I}_A \cdot \tilde{I}_B < 0$ appear.

Because of the injected signal from A, the intensity in B changes to $I'_B = I_B + \gamma I_A$; i.e., system B experiences a total feedback power larger than system A. As a consequence of the saturation of the nonlinearity, this causes a difference between A and B. In order to reduce this effect, a uniform bias beam was superimposed onto A, such that $I'_A = I_A + I_{\text{bias}}$ with $I_{\text{bias}} = \gamma\langle I_A\rangle_x$, where the brackets $\langle\cdot\rangle_x$ denote spatial averaging. The seemingly simpler attenuation of I'_B was hindered by technical reasons.

With the spatial low-pass filter cutoff set just above the fundamental critical wave number, the pump intensity I_p was set to different values above the pattern forming threshold I_{th}. An additional measurement series was carried out with open low pass and the pump at $I_p = 1.5 I_{\text{th}}$. In each particular measurement, the coupling strength was set to a fixed value and a temporal image sequence of up to 100 s duration was recorded.

From each sequence, we computed a spatial cross-correlation function between A and B

$$C(\Delta\mathbf{x}, \Delta t, t) = \frac{\langle \tilde{I}_A(\mathbf{x}, t) \cdot \tilde{I}_B(\mathbf{x} - \Delta\mathbf{x}, t - \Delta t)\rangle_x}{\sqrt{\langle \tilde{I}_A^2(\mathbf{x}, t)\rangle_x \langle \tilde{I}_B^2(\mathbf{x}, t)\rangle_x}}, \qquad (1)$$

where $\mathbf{x}$ denotes the transverse coordinates and I_A and I_B are the experimentally recorded intensity distributions of master and slave systems, respectively. The tildes stand for the deviation from the mean value $\tilde{I} = I - \langle I\rangle_x$. Boundary effects are excluded by considering only the central parts of the active areas (85% of the diameter).

We find a synchronization, where the slave state follows the master with a certain time lag — an effect known from purely temporal systems [1]. The left panel of Fig. 4 presents typical examples of correlation functions: The peaks appear at a time lag $\Delta t = -\tau_l(\gamma)$. It is also

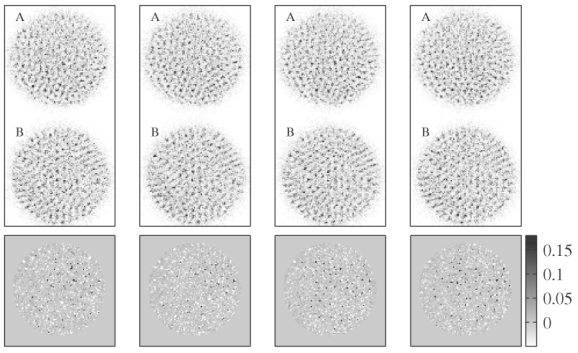

FIG. 3. As in Fig. 2, but here with open low-pass filter and the snapshots taken at time intervals of $t = 0.2$ s.

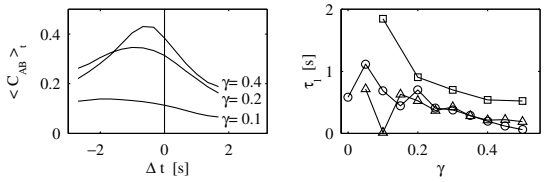

FIG. 4. Left panel: Typical examples for the time-averaged correlation $\langle C_{AB}(0, 0, \Delta t, t)\rangle_t$, derived for the pump intensity at 1.5 times and closed low-pass filter. Right panel: Dependence of the time lag τ_l on coupling strength γ. □, $I_p = 1.5I_{\text{th}}$; ○, $I_p = 3I_{\text{th}}$, both for closed low pass; △, $I_p = 1.5I_{\text{th}}$ with open low pass.

typical that the peak correlations are about 20% larger than at $\Delta t = 0$. The time lag τ_l is found to drop with increasing coupling strength (Fig. 4, right panel). A spatial counterpart of the time lag would be a lateral shift (or rotation) between the two patterns. Such a lateral shift, however, was not observed; the dominant correlation peak always appears at $\Delta\mathbf{x} = (0, 0)$, independently of Δt.

Consequently, we use the correlation coefficient $c_{AB}(t) = C(0, 0, \tau_l, t)$ as a measure for synchronization. The left panel of Fig. 5 shows the time-averaged correlation coefficients, plotted over the coupling factor γ. The error bars indicate the rms value of the temporal variation. We have checked that the correlation coefficients do not show temporal drifts, which confirms that the coupled systems were in their asymptotic states.

The increase of c_{AB} with the coupling strength γ clearly substantiates that the two systems become synchronized by the coupling. Because of experimental imperfections and remaining differences between the systems A and B, the correlation coefficient never reaches unity. The fact that the correlation drops again at larger coupling strengths can be assigned to the increasing difference between the systems: The bias intensity for the master system A is an insufficient way to balance the unidirectional coupling. Figure 5 also shows that, further above threshold, where the structures are more disordered, synchronization is harder to achieve.

Snapshots of synchronized states are presented in Fig. 6, for the pump intensity just above threshold and closed low-pass filter. The bottom panels show the local correlations $\tilde{I}_A \cdot \tilde{I}_B$, visualizing that the two structures correspond to each other in large parts. Without coupling instead, the two systems A and B are independent, as can be taken from Fig. 2.

As an alternative measure, we have computed the mutual information $M_{AB} = H_A + H_B - H_{AB}$ (Fig. 5, right panel). The entropies $H_{..} = \sum p_{..} \log_2 p_{..}$ depend on the (joint) probability distributions $p_{..}$ of the intensities I_A and I_B. We have used a histogram based method with fixed and equal bins and have renounced on a correction of the bias caused by the sampling [18]. This is sufficient, since we are mainly interested in the dependence on γ. The recorded intensities were reduced to a resolution of 5 bits as a compromise between fine sampling of the probability distributions and sufficient counts per histogram bin. To enlarge the data basis, the probability distributions were determined from the whole image sequence, and not for each snapshot individually. The error bars indicate the estimated error, as described in [18]. In all cases, the mutual information increases with γ, again indicating a coupling-induced synchronization.

Without low-pass filtering, a larger number of critical wave number bands contributes to the pattern formation process, resulting in very complex and dynamic structures (cf. Fig. 3). In this case, the maximum achievable correlation coefficient and mutual information are rather low and already saturate for $\gamma \geq 0.2$ (cf. Fig. 5). The reduced synchronization is probably the consequence of the increased sensitivity to perturbations. Without low-pass filtering, the system supports a much broader bandwidth and, consequently, spatial noise gains more influence. However, the increase of the correlation and of the mutual information at lower coupling strengths still gives evidence for a partial, coupling-induced synchronization.

For comparison, numerical simulations of the full model equations were carried out, focusing on the effect of spatial inhomogeneities. It is difficult to quantify the experimental imperfections exactly. In particular, their spatial profiles and/or spatial frequency spectra play a decisive role. We have already observed that the transition to and the characteristics of spatial complexity depend sensitively on the inhomogeneities [11,19]. Hence, the presented simulations are based on several assumptions

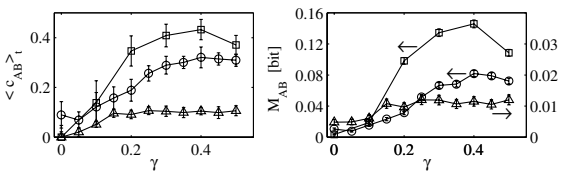

FIG. 5. Left panel: Time-averaged correlation coefficient $\langle c_{AB}\rangle_t$; right panel, mutual information M_{AB}. □, pump intensity set to $I_p = 1.5I_{\text{th}}$; ○, to $I_p = 3I_{\text{th}}$, both for closed low pass; △, $I_p = 1.5I_{\text{th}}$ with open low pass.

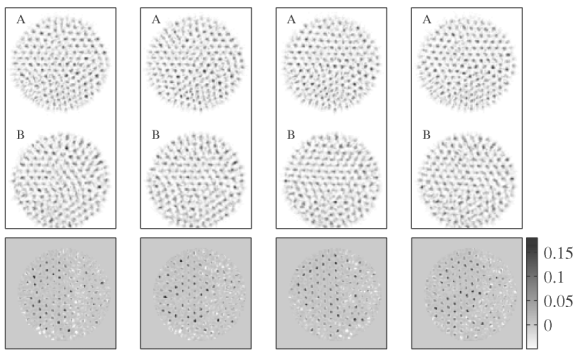

FIG. 6. Synchronized states at $\gamma = 0.4$; the other system parameters and the gray scales correspond to Fig. 2. Master and slave images are taken simultaneously, i.e., for $\Delta t = 0$.

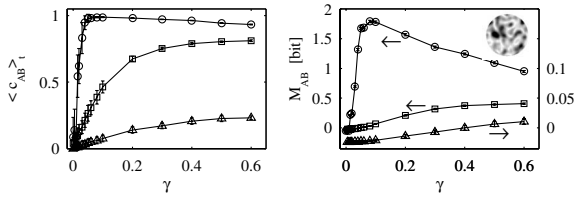

FIG. 7. Correlation coefficient c_{AB} (left panel), and mutual information M_{AB} (right panel) from numerical simulations with no (□), small (○), and strong inhomogeneities (△). The inset shows a typical profile of the nonlinear sensitivity.

and give only a qualitative picture. We use the scheme described in [11], including speckles in the pump light and spatial variations of the nonlinear sensitivity — both different for master and slave. A grid of 128^2 points was used at a pump intensity of 3 times threshold with realistic circular boundaries and no low-pass filter. To simulate speckles, we added white spatial noise to the pump beam (fraction f of the total power in nonzero Fourier modes). The nonlinear sensitivities were given smooth random profiles with an rms variation of σ.

Figure 7 shows the resulting correlation coefficients and mutual information for no ($f = \sigma = 0$), small ($f = \sigma = 2\%$), and stronger inhomogeneities ($f = \sigma = 5\%$). Clearly, the amount of synchronization declines with increasing strength of the inhomogeneities. In Fig. 7, one can find again the decay of high synchronization with γ, as already observed in the experiment and assigned to the growing difference between master and slave.

In conclusion, we have found evidence for a time-lag synchronization of spatiotemporal disorder in a nonlinear-optical experiment, realized in a unidirectionally coupled master-slave configuration. The increase of the cross correlation and the mutual information with the coupling strength clearly indicate coupling-induced synchronization. The time lag between master and slave state was observed to decrease with coupling strength. Corresponding numerical simulations reveal how spatial inhomogeneities counteract synchronization, which can explain the imperfect experimental synchronization.

The mechanisms of this *synchorization* (from $\chi\omega\rho\iota\sigma\nu$: place) of spatiotemporal disorder appear to be quite general; an observation in other nonlinear extended systems should be possible. Good candidates, besides other nonlinear-optical systems, are photosensitive chemical reaction-diffusion systems, which can both be detected and manipulated with light waves. A necessary translation between detection and controlling light or an amplification of the detection light can be performed by means of optically addressable spatial light modulators [13].

The authors would like to thank R. Roy and J. García-Ojalvo for inspiring discussions, and acknowledge the support by T. Tschudi and Jenoptik LOS GmbH, Jena.

[1] A. Pikovsky, M. Rosenblum, and J. Kurths, *Synchronization* (Cambridge University Press, Cambridge, England, 2001); S. Boccaletti *et al.*, Phys. Rep. **366**, 1 (2002).
[2] M. C. Cross and P. C. Hohenberg, Rev. Mod. Phys. **65**, 851 (1993).
[3] M. A. Vorontsov and W. B. Miller, *Self-Organization in Optical Systems and Applications in Information Technology* (Springer-Verlag, Berlin, 1995); L. A. Lugiato, M. Brambilla, and A. Gatti, Adv. At. Mol. Phys. **40**, 229 (1998); F. T. Arecchi, S. Boccaletti, and P. L. Ramazza, Phys. Rep. **318**, 83 (1999).
[4] P. Parmananda, Phys. Rev. E **56**, 1595 (1997); A. Amengual, E. Hernandez-Garcia, R. Montagne, and M. San Miguel, Phys. Rev. Lett. **78**, 4379 (1997); J. García-Ojalvo and R. Roy, Phys. Rev. Lett. **86**, 5204 (2001).
[5] S. Boccaletti, J. Bragard, F. T. Arecchi, and H. Mancini, Phys. Rev. Lett. **83**, 536 (1999).
[6] L. Kocarev, Z. Tasev, and U. Parlitz, Phys. Rev. Lett. **79**, 51 (1997); S. Boccaletti, J. Bragard, and F. T. Arecchi, Phys. Rev. E **59**, 6574 (1999); L. Junge and U. Parlitz, Phys. Rev. E **61**, 3736 (2000).
[7] G. D'Alessandro and W. J. Firth, Phys. Rev. A **46**, 537 (1992).
[8] R. Macdonald and H. J. Eichler, Opt. Commun. **89**, 289 (1992); M. Tamburrini, M. Bonavita, S. Wabnitz, and E. Santamato, Opt. Lett. **18**, 855 (1993); G. Grynberg, A. Maître, and A. Petrossian, Phys. Rev. Lett. **72**, 2379 (1994); T. Ackemann, Y. A. Logvin, A. Heuer, and W. Lange, Phys. Rev. Lett. **75**, 3450 (1995); T. Honda *et al.*, Opt. Commun. **133**, 293 (1997).
[9] F. T. Arecchi *et al.*, J. Nonlinear Opt. Phys. Mater. **9**, 183 (2000).
[10] R. Neubecker, G.-L. Oppo, B. Thuering, and T. Tschudi, Phys. Rev. A **52**, 791 (1995); B. Thüring *et al.*, Asian J. Phys. **7**, 453 (1998).
[11] R. Neubecker and E. Benkler, Phys. Rev. E **65**, 066206 (2002).
[12] S. A. Akhmanov *et al.*, J. Opt. Soc. Am. B **9**, 78 (1992); M. A. Vorontsov, N. G. Iroshnikov, and R. L. Abernathy, Chaos Solitons Fractals **4**, 1701 (1994).
[13] *Spatial Light Modulator Technique*, edited by U. Efron (Marcel Dekker, New York, 1995); N. Hawlitschek, P. Gärtner, P. Gussek, and F. Reichel, Exp. Techn. Phys. **40**, 199 (1994).
[14] R. Neubecker, B. Thüring, M. Kreuzer, and T. Tschudi, Chaos Solitons Fractals **10**, 681 (1999); G. Schliecker and R. Neubecker, Phys. Rev. E **61**, R997 (2000).
[15] M. A. Vorontsov, J. C. Ricklin, and G.W. Carhart, Opt. Eng. **34**, 3229 (1995); P. L. Ramazza, S. Ducci, S. Boccaletti, and F. T. Arecchi, J. Opt. B **2**, 399 (2000).
[16] M. Le Berre, A. S. Patrascu, E. Ressayre, and A. Tallet, Phys. Rev. A **56**, 3150 (1997).
[17] R. Neubecker and A. Zimmermann, Phys. Rev. E **65**, 035205(R) (2002); R. Neubecker and O. Jakoby, Phys. Rev. E **67**, 066221 (2003).
[18] M. S. Roulston, Physica (Amsterdam) **125D**, 285 (1999).
[19] R. Neubecker, E. Benkler, R. Martin, and G.-L. Oppo, Phys. Rev. Lett. **91**, 113903 (2003).